Theoretical study of direct-current and radio-frequency breakdown in GaN wurtzite- and zinc-blende-phase MESFETs (metal-semiconductor field-effect transistors)

2001 J. Phys.: Condens. Matter 13 10477

(http://iopscience.iop.org/0953-8984/13/46/316)

INSTITUTE OF PHYSICS PUBLISHING JOURNAL OF PHYSICS: CONDENSED MATTER

J. Phys.: Condens. Matter **13** (2001) 10477–10486 PII: S0953-8984(01)28201-0

Theoretical study of direct-current and radio-frequency breakdown in GaN wurtzite- and zinc-blende-phase MESFETs (metal–semiconductor field-effect transistors)

Maziar Farahmand[1], **Michael Weber**[2], **Louis Tirino**[2], **Kevin F Brennan**[2] **and P Paul Ruden**[3]

[1] Movaz Networks, One Technology Parkway, South Norcross, GA 30092, USA
[2] School of Electrical and Computer Engineering, Georgia Tech, Atlanta, GA 30332-0250, USA
[3] Department of Electrical and Computer Engineering, University of Minnesota, Minneapolis, MN 55455, USA

Received 22 August 2001
Published 2 November 2001
Online at stacks.iop.org/JPhysCM/13/10477

Abstract

In this paper, we present a comparison of the direct-current (DC) and radio-frequency (RF) breakdown behaviours of representative wurtzite- and zinc-blende-phase GaN MESFET structures based on a theoretical analysis. The calculations are made using a full-band ensemble Monte Carlo simulation that includes a numerical formulation of the impact ionization transition rate. Calculations of both the DC and RF breakdown voltages are presented for submicron MESFET devices made from either wurtzite- or zinc-blende-phase GaN. The devices are otherwise identical. It is found that the DC breakdown voltage in the wurtzite-phase GaN MESFET is significantly larger than that in the zinc-blende-phase device. This is due to the fact that electron heating occurs more rapidly within the zinc-blende phase than the wurtzite phase of GaN. As a consequence, avalanche breakdown occurs at higher applied field strengths and voltages in the wurtzite phase than in the zinc-blende phase of GaN. It is further found that the RF breakdown voltage of the devices increases with increasing frequency of the applied large-signal RF excitation.

1. Introduction

The wide-band-gap semiconductors offer much promise for future high-power, high-frequency device applications [1–3]. Owing to their wide energy band gaps, these materials are less susceptible to high-field-induced breakdown than conventional silicon or GaAs-based devices. Coupled with a higher saturation drift velocity, the high breakdown field strengths of the wide-band-gap semiconductors offer a significant expansion of the power–frequency coverage range

over existing technologies. The higher power-density levels that these materials can deliver also provide the opportunity for significant miniaturization.

Of the many different wide-band-gap semiconductor materials, the group III nitrides, and in particular GaN, are gaining prominence. GaN crystallizes into two different polytypes, wurtzite (WZ) with hexagonal symmetry and zinc-blende (ZB) with cubic symmetry. The crystal morphology depends upon substrate choice and growth conditions. GaN is particularly attractive for device applications since it can form type I heterojunctions with related group III nitride ternary compounds. The formation of type I heterojunctions enables exploitation of modulation doping and consequently the creation of MODFET (modulated field-effect transistor) devices. Additionally, the lattice mismatch between GaN and the ternary compound AlGaN in appropriately designed structures produces strain-induced polarization fields [4, 5]. These strain-induced polarization fields can alter the band bending and carrier concentration at the heterointerface, providing a new degree of device engineering.

Given the potential of the III nitrides for use in high-power electronics, it is important to characterize their properties and device behaviour. Unfortunately, the technological immaturity of the III nitride materials systems, owing primarily to the lack of suitable substrate material, has slowed experimental evaluation of III-nitride-based devices. In order to help facilitate the process of evaluating the device potential of the wide-band-gap semiconductors and in particular the III nitrides, we have developed a theoretical modelling tool that can operate relatively independently of experimental investigation. This approach is referred to as materials-theory-based modelling [6–8]. The full details of the method have been exhaustively reported elsewhere [6–8]. A key ingredient within the materials-theory-based modelling method is the full-band ensemble Monte Carlo simulation [9]. The full-band Monte Carlo model is particularly attractive for studying materials such as the wide-band-gap semiconductors where definitive transport properties have not been established. We have applied the materials-theory-based modelling method to the study of the bulk properties of GaN [10, 11], 3C-SiC [12], 4H-SiC [13], InN [14] and the ternary III nitride compounds [15]. Recent experimental measurements show good agreement with the breakdown properties of GaN predicted by materials theory modelling [16], thus confirming the basic validity of the approach.

In addition, we have examined the device potential of the III nitride materials using an extension of the materials-theory-based modelling method [17, 18] on the basis of a self-consistent full-band Monte Carlo simulation. The device structures investigated were submicron-gate-length MESFETs. Both the DC breakdown and frequency performance of these devices were examined.

The materials-theory-based modelling method has been useful in examining how the transport and device potentials of the two polytypes of GaN compare. It has been found that, owing to the difference in band structure, the bulk and device performances of wurtzite and zinc-blende GaN are substantially different [11, 18]. Specifically, the DC breakdown voltages of wurtzite- and zinc-blende-phase GaN MESFETs have been predicted to be substantially different [18]. Knowledge of the breakdown properties of a device is critical in evaluating the maximum output power for a class A amplifier. A class A amplifier has a maximum output power given as

$$P_{\max} = \frac{(V_{\mathrm{BR}} - V_{\mathrm{knee}})^2}{8R_{\mathrm{L}}} \tag{1}$$

where V_{BR} is the breakdown voltage, V_{knee} the knee voltage defined as the voltage at which the transistor current saturates, and R_{L} is the load resistance. Obviously, the larger the difference between the knee and breakdown voltages, the greater the maximum output power that the

device can deliver. The knee voltage is a function of the mobility. A higher mobility results in a smaller value of V_{knee}. The breakdown voltage is a strong function of the energy gap. Wider-band-gap materials have higher breakdown voltages. Though the energy band gaps of the wurtzite and zinc-blende phases of GaN are close in magnitude, the breakdown electric field strengths are significantly different. The difference in breakdown electric field strength is attributable to the difference between the properties of the wurtzite and zinc-blende band structures that results in different carrier temperatures within the two materials.

The breakdown voltage has also been experimentally found to depend upon RF conditions. It has been observed that under large-signal high-frequency conditions, devices can be driven beyond their DC breakdown limits [19, 20]. The breakdown voltage under RF conditions is higher than that under DC conditions, thus implying that the maximum output power can be greater under RF excitation. Recently, we have examined the RF dependence of the breakdown voltage of zinc-blende-phase GaN MESFETs [21]. It was found that the breakdown voltage under RF driving is frequency dependent; however, no comparison of the RF breakdown behaviour of the different polytypes of GaN was presented. It is the purpose of this paper to present calculated results for both DC and RF breakdown in MESFETs using both the wurtzite and zinc-blende polytypes of GaN. It is expected that the physical implications derived from the calculations presented herein could have impact on circuit-level designs of high-power, high-frequency amplifiers relevant to future wireless communications networks.

2. Model description

The calculations are made using a two-dimensional real-space self-consistent full-band ensemble Monte Carlo simulation. The full details of the approach have been presented elsewhere [17] and will not be repeated here. The geometry and doping concentrations of the simulated MESFET device are shown in figure 1. The small dimensions of the device have been chosen to limit the computational demands of the simulator. Owing to the large number of simulated particles and the relatively long simulation times needed to ensure numerical accuracy, a larger device than that chosen here is currently unrealistic. The donor doping level of 3×10^{17} cm^{-3} is typical for GaN devices. All the simulations are performed assuming a constant ambient temperature of 300 K. The dopants are all assumed to be fully ionized and with no doping compensation present.

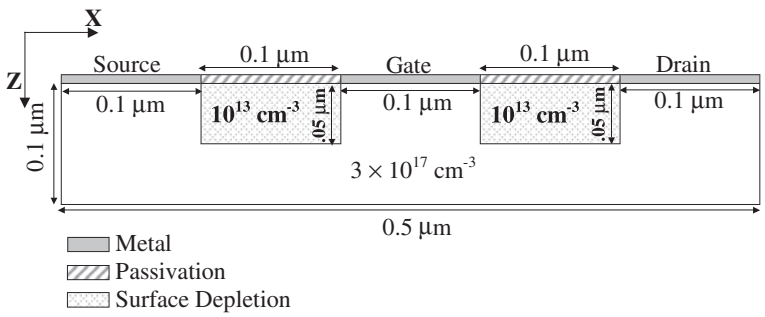

Figure 1. The cross section of the MESFET.

Though much progress has been made in the growth of GaN, current state-of-the-art material is still plagued by large concentrations of defects. In addition, passivation of the material is currently poorly controlled, resulting in the introduction of surface states. In order

to account for the effect of these surface states on device performance, the device is modelled with two surface-state-depletion regions formed between the source and gate and the drain and gate as shown in figure 1. It is assumed that the surface states act to deplete out the underlying semiconductor layer, resulting in a carrier concentration of 10^{13} cm^{-3} as shown. For simplicity, the depleted region is assumed to be rectangular with a depth equal to half the GaN active-layer thickness and a length equal to the source–gate and drain–gate separations. In both the DC and RF calculations, the surface-state-depletion condition is assumed.

Aside from the obvious differences in the band structures and the associated phonon and impact ionization rates, the MESFET simulations for the wurtzite and zinc-blende phases are essentially identical. Treatment of band crossing and mixing points for the wurtzite-phase device is performed following the approach outlined in reference [18].

The MESFET simulation is inherently unipolar. Holes are not included within the simulation. This approximation is expected to be valid until the secondary hole concentration becomes non-negligible, which occurs after breakdown. However, the definition of breakdown in the absence of the holes becomes somewhat arbitrary. The breakdown voltage under either DC or RF conditions must then be defined. In this work, the breakdown voltage is defined as the drain–source voltage for which the drain current calculated with impact ionization is 3% higher than the drain current calculated without impact ionization. This definition is used to define the occurrence of breakdown under DC conditions.

The breakdown characteristics of the wurtzite- and zinc-blende-phase GaN MESFETs are also compared under RF operation. A large-signal RF bias is applied between the drain and source, simulating on-state breakdown. Though in most common source configurations the RF signal is applied to the gate, this situation is more difficult and computationally expensive to simulate using the Monte Carlo method. The RF breakdown results that we present are nevertheless useful in examining the effect on the breakdown voltage of RF excitation, since the frequency dependence of the carrier heating is somewhat independent of the bias condition. The waveform applied to the drain contact is assumed to be sinusoidally varying between high and low voltages, $V_{\rm hi}$ and $V_{\rm lo}$, respectively, with angular frequency, ω. The drain current is again calculated under two conditions, with and without impact ionization, in order to determine the breakdown conditions.

The RF breakdown voltage for both the wurtzite and zinc-blende MESFET structures is determined as follows. In an earlier investigation [21] we found that for the zinc-blende-phase GaN MESFET the device is in the breakdown condition defined above (3% difference between the drain currents calculated with and without impact ionization present) under a large-signal RF voltage described by

$$V_{\rm ds}(t) = 17.5 + 12.5\cos(\omega t) \tag{2}$$

with a frequency of 80 GHz. In our earlier investigation [21], it was determined that the device is in the breakdown condition when the voltage swings between $V_{\rm hi} = 30$ V and $V_{\rm lo} = 5$ V at a frequency of 80 GHz. The value of $V_{\rm hi}$ is greater than the DC breakdown voltage of the zinc-blende-phase device, 24 V. The frequency of the RF signal is then increased until the device no longer exhibits breakdown. The corresponding frequency is termed the onset breakdown frequency. A similar procedure is used for the wurtzite-phase device and the frequency at which the onset of breakdown occurs is compared.

3. Calculated DC breakdown of GaN MESFETs

The calculated drain currents, $I_{\rm d}$, versus drain–source voltage, $V_{\rm ds}$, for gate–source voltage, $V_{\rm gs}$, varying from -0.1 to -5.1 V in 1 V steps for both the zinc-blende- and wurtzite-phase

devices are shown in figure 2. The Schottky barrier potential height is included in V_{gs}. The drain current at each bias point is determined both with and without impact ionization. The solid and dotted lines in figure 2 represent the calculated drain current in the presence and absence of impact ionization respectively. The relatively high output conductance of the devices is a consequence of the small gate length. Inspection of figure 2 shows that the DC breakdown voltage is significantly higher in the wurtzite-phase device than in the zinc-blende-phase device under all gate bias conditions. For example, the breakdown voltage at a gate–source bias of -0.1 V is 25 V for the zinc-blende device compared with 45 V for the wurtzite device under the same gate–source bias. The nature of this sizable difference in breakdown voltage can be understood as follows.

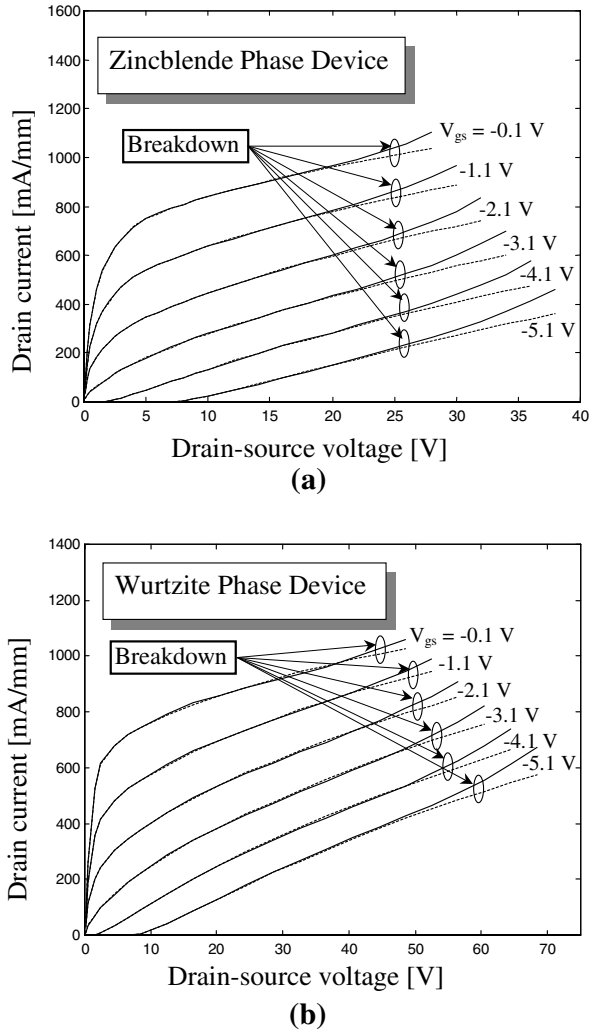

Figure 2. Output characteristics for the zinc-blende-phase device (a) and the wurtzite-phase device (b). The gate–source voltage, V_{gs}, includes the Schottky barrier height. The drain currents have been calculated with impact ionization (solid lines) and without impact ionization (dashed lines). The ovals show the breakdown locations on the I–V curves. The breakdown voltage is calculated according to the convention discussed in the text.

The difference in energy gap between the wurtzite and zinc-blende phases of GaN is only about 5%. Such a small difference in band gap cannot by itself account for the sizable difference in predicted breakdown voltage. Earlier calculations also predicted a sizable difference between the impact ionization coefficients for bulk zinc-blende- and wurtzite-phase GaN [10]. Impact ionization is a threshold process. The coefficients depend upon two processes: the rate at which the carriers reach the threshold condition for impact ionization and the ionization transition rate at and above threshold [22]. The ionization transition rate as a function of energy in both zinc-blende and wurtzite GaN was calculated by Kolnik *et al* [23]. They found that the transition rate in the zinc-blende phase is systematically only slightly higher than that in the wurtzite phase throughout the full range of energies examined. Therefore, the marked difference between the calculated ionization coefficients is believed to be due primarily to the difference between the rates at which the carriers achieve the threshold for impact ionization. Subsequent calculations of the ionization coefficients [10, 11] have shown that the electron distribution is much 'cooler' within the wurtzite phase than the zinc-blende phase of GaN at comparable electric field strengths. Therefore, at a given field strength fewer electrons achieve threshold in wurtzite GaN than in zinc-blende GaN, resulting in a lower ionization coefficient for wurtzite GaN. The higher breakdown voltage of the wurtzite-phase device is thus attributable to the difference in carrier temperature between the wurtzite and zinc-blende phases of GaN. The density of states within wurtzite GaN is greater than that within zinc-blende GaN. As a result of the greater electronic density of states, the electrons are, on average, 'cooler' in the wurtzite phase than in the zinc-blende phase under the same bias conditions.

4. Calculated RF breakdown of GaN MESFETs

The RF breakdown dependency is studied by applying a DC bias on the gate, V_{gs}, of -0.1 V with an RF voltage, V_{ds}, described by equation (2) applied to the drain with the source grounded. The device dimensions and doping concentrations are the same as those used for the DC calculations. Both wurtzite- and zinc-blende-phase GaN devices are examined. The breakdown behaviour is an obvious function of the bias conditions and has been found to also depend upon the frequency of the RF excitation [21]. The earlier calculations made on the zinc-blende-phase MESFET are used as a starting point in these investigations. In reference [21] the bias conditions for the zinc-blende-phase MESFET are adjusted such that the device is in the breakdown condition as defined above at a frequency of 80 GHz with the applied RF voltage swing given by equation (2). In the calculations presented here, we are mainly interested in determining at what frequency the device is no longer in the breakdown condition for a given excitation. Owing to the inherent uncertainty of the drain currents generated by Monte Carlo simulation, it is best to select a baseline bias condition such that the calculated drain currents with and without impact ionization are significantly different. To this end, we have chosen to use as a starting point a frequency of 20 GHz with the applied voltage specified by equation (2) for the zinc-blende device. The applied RF bias in the zinc-blende device is such that $V_{hi} = 30$ V and $V_{lo} = 5$ V. The resulting calculated drain current is shown in figure 3. The solid lines in the figure show the calculated drain current with impact ionization present and the dashed lines show the drain current in the absence of impact ionization. Inspection of the top panel of figure 3 reveals that at the RF of 20 GHz, the device is well beyond breakdown; the drain currents with and without impact ionization differ by about $\sim$8.5%, significantly larger than the 3% referred to above used to define the breakdown condition. As the frequency is increased, the device ultimately is no longer in the breakdown condition. The actual frequency at which the breakdown disappears, defined as the condition where the calculated drain currents with and without impact ionization become the same, is difficult to accurately assess due to

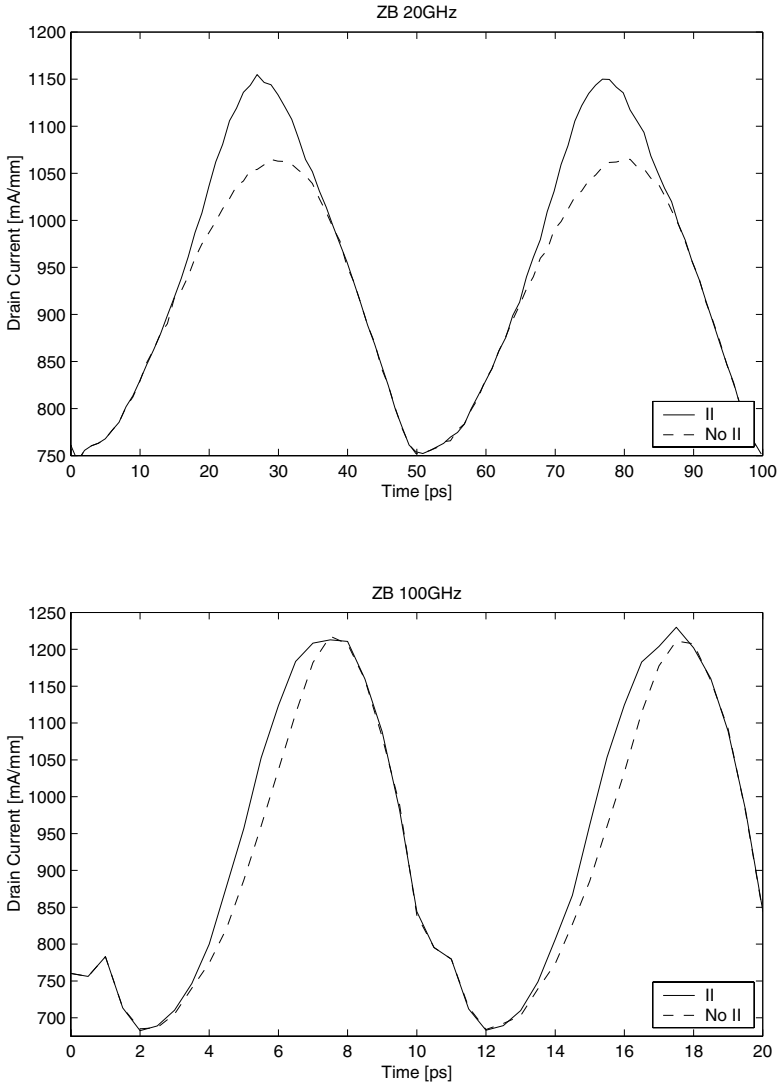

Figure 3. Calculated electron drain current as a function of time with (solid line) and without (dashed line) impact ionization for the zinc-blende-phase GaN MESFET at an excitation frequency of (top panel) 20 GHz and (bottom panel) 100 GHz.

the inherent uncertainty in the currents calculated from Monte Carlo simulation. Nevertheless, the onset frequency for breakdown lies somewhere in the frequency range between 95 and 100 GHz for the given bias conditions for the zinc-blende GaN MESFET. For purposes of illustration, we present the calculated results for a frequency of 100 GHz in the bottom panel of figure 3.

It is interesting to compare the breakdown behaviours of the wurtzite and zinc-blende GaN MESFETs under RF drive. As discussed in section 3, the DC breakdown voltages are different for the wurtzite- and zinc-blende-phase devices. The applied gate–source voltage is -0.1 V, the same as for the zinc-blende-phase MESFET. Consequently, the RF voltage applied to the drain must necessarily swing through a higher voltage for the wurtzite-phase device than

for the zinc-blende-phase device at a RF of 20 GHz. To achieve the same relationship of the calculated drain currents as in the zinc-blende device, the bias that must be applied to the drain of the wurtzite device is

$$V_{ds}(t) = 31 + 26\cos\omega t. \tag{3}$$

The resulting calculated drain currents with and without impact ionization for the wurtzite-phase device are shown in the top panel of figure 4 at a RF of 20 GHz. Comparison of the top panels of figures 3 and 4 shows that the ZB- and WZ-phase devices operate at about the same breakdown point under these conditions. As the frequency is increased, breakdown within the wurtzite device also disappears. In this case, the frequency range at which the device is no longer in the breakdown condition is calculated to be 55–60 GHz. For illustration purposes, the calculated drain currents for an excitation RF of 60 GHz are illustrated in the bottom panel of figure 4.

Interestingly, the frequency at which the device no longer exhibits breakdown is lower for the wurtzite-phase device than the zinc-blende-phase device. A possible explanation of this observation is given as follows. In our earlier investigation of RF breakdown [21] it was suggested that as the frequency of the excitation increases, the electrons can no longer fully respond to the changing electric field. As a result, their energy and consequently their ionization coefficient approach an intermediate value between the two extremes produced by the high- and low-field components of the RF signal. Thus at some frequency the carriers experience an average field strength that, depending upon the RF signal magnitude, is below that needed for breakdown. Here we have further determined that there is a difference between the frequencies for which the device is no longer in the breakdown condition for WZ- and ZB-phase GaN devices. It is found that the frequency is lower in the WZ-phase device than the ZB-phase device when the device ceases to exhibit breakdown. We speculate that the physical explanation of this effect is that the electrons in WZ GaN cannot follow the signal as rapidly as electrons in ZB GaN. We believe that this is again due to the difference in density of states between the two phases, resulting in a somewhat greater electron inertia in WZ than in ZB. It should be noted that a definitive explanation is currently lacking, pending further investigations of the breakdown behaviour of devices made using other materials systems. Such a study will be reported in a future work.

5. Conclusions

In this paper, we have presented ensemble, full-band, self-consistent Monte Carlo calculations of the DC and RF breakdown behaviour of otherwise identical zinc-blende- and wurtzite-phase GaN MESFETs. It is found that the DC breakdown voltage of the wurtzite-phase device is significantly greater than that of the zinc-blende-phase MESFET structure. The calculated difference in breakdown voltage is attributed primarily to the difference between the rates at which the carriers achieve the threshold energy for impact ionization. The electron distribution is much 'cooler' within the wurtzite phase than the zinc-blende phase of GaN at comparable electric field strengths. Consequently, a higher electric field strength is required to heat the electrons to the ionization threshold energy in wurtzite GaN.

Investigation of the RF breakdown behaviour of wurtzite- and zinc-blende-phase GaN MESFETs shows that the breakdown voltage in both materials is highly sensitive to the excitation RF. As the frequency increases, the RF breakdown voltage increases. As the RF increases, the electrons can no longer fully respond to the changing electric field. As a result, the electron energy and consequently the impact ionization coefficient are lowered, thereby increasing the breakdown voltage of the device. It is further found that a

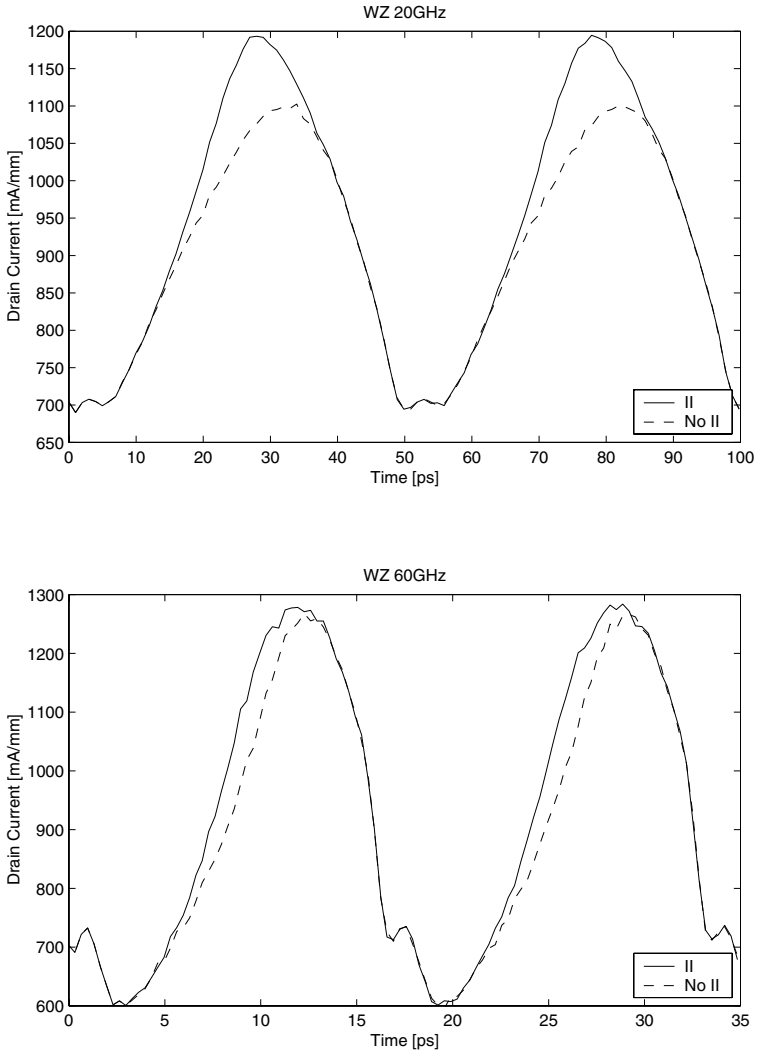

Figure 4. Calculated electron drain current as a function of time with (solid line) and without (dashed line) impact ionization for the wurtzite-phase GaN MESFET at an excitation RF of (top panel) 20 GHz and (bottom panel) 60 GHz.

higher-frequency change is required in the ZB phase than the WZ phase to eliminate breakdown in the corresponding MESFET structures.

It is suggested that the difference in RF breakdown voltage arises from the difference between the electron dynamics within the ZB and WZ phases. The electrons within WZ GaN cannot follow the signal frequency as rapidly as electrons in ZB GaN. Consequently, the electrons in WZ GaN settle at an average electric field strength, depending upon the magnitude of the applied RF signal, less than the breakdown field strength of the device at a lower frequency than in ZB GaN. It is further speculated that this is physically a consequence of the difference in electron inertia, or more generally density of states, between the two phases. Further investigation of the RF breakdown properties of other materials is needed to clarify this point.

From the results presented in this paper it is clear that the breakdown properties of wurtzite- and zinc-blende-phase GaN are very different. The DC maximum output power is predicted to be greater for wurtzite GaN devices than zinc-blende devices. Under RF conditions, the breakdown voltage for either phase of GaN is found to be frequency dependent. It is further found that a greater excitation frequency is required in the ZB phase than the WZ phase in order to eliminate breakdown. It is expected that these results could have an impact on device selection and circuit-level designs of high-power, high-frequency amplifiers for future wireless communications systems.

Acknowledgments

This work was sponsored in part by the National Science Foundation through Grant ECS-9811366, the Office of Naval Research through Contract E21-K19, and the Yamacraw Initiative.

References

[1] Eastman L F 1999 *Phys. Status Solidi* a **176** 175
[2] Shur M S 1998 *Solid-State Electron.* **42** 2131
[3] Trew R J 1998 *Semiconductors and Semimetals* vol 52, ed R K Willardson and A C Beer (New York: Academic) p 237
[4] Smith D L 1986 *Solid-State Commun.* **57** 919
[5] Ambacher O, Foutz B, Smart J, Shealy J R, Weimann N G, Chu K, Murphy M, Sierakowski A J, Schaff W J, Eastman L F, Dimitrov R, Mitchell A and Stutzmann M 2000 *J. Appl. Phys.* **87** 334
[6] Brennan K F, Bellotti E, Farahmand M, Haralson J II, Ruden P P, Albrecht J D and Sutandi A 2000 *Solid-State Electron.* **44** 195
[7] Brennan K F, Kolnik J, Oguzman I H, Bellotti E, Farahmand M, Ruden P P, Wang R and Albrecht J D 2000 *GaN and Related Materials II* vol 7, ed S J Pearton (Sydney: Gordon and Breach) 305
[8] Brennan K F, Bellotti E, Farahmand M, Nilsson H-E, Ruden P P and Zhang Y 2000 *IEEE Trans. Electron Devices* **47** 1882
[9] Shichijo H and Hess K 1981 *Phys. Rev.* B **23** 4197
[10] Kolnik J, Oguzman I H, Brennan K F, Wang R and Ruden P P 1997 *J. Appl. Phys.* **81** 726
[11] Oguzman I H, Bellotti E, Brennan K F, Kolnik J, Wang R and Ruden P P 1997 *J. Appl. Phys.* **81** 7827
[12] Bellotti E, Nilsson H-E, Brennan K F and Ruden P P 1999 *J. Appl. Phys.* **85** 3211
[13] Bellotti E, Nilsson H-E, Brennan K F, Ruden P P and Trew R 2000 *J. Appl. Phys.* **87** 3864
[14] Bellotti E, Doshi B K, Brennan K F, Albrecht J D and Ruden P P 1999 *J. Appl. Phys.* **85** 916
[15] Farahmand M, Garetto C, Bellotti E, Brennan K F, Goano M, Ghillino E, Ghione G, Albrecht J D and Ruden P P 2001 *IEEE Trans. Electron Devices* **48** 535
[16] Verghese S, McIntosh K A, Molnar R J, Mahoney L J, Aggarwal R L, Geis M W, Molvar K M, Duerr E K and Melngailis I 2001 *IEEE Trans. Electron Devices* **48** 502
[17] Farahmand M and Brennan K F 1999 *IEEE Trans. Electron Devices* **46** 1319
[18] Farahmand M and Brennan K F 2000 *IEEE Trans. Electron Devices* **47** 493
[19] Heo D, Yoo S, Chen E, Gebara E, Hamai M and Laskar J 2000 *Proc. IEEE Int. Microwave Symp. (Boston, MA)*
[20] Tkachenko Y A, Wei C J and Hwang J C M 1996 *Proc. 47th ARFTG Conf. (San Francisco, CA)* digest, p 67
[21] Farahmand M, Brennan K F, Gebara E, Heo D, Suh Y and Laskar J 2001 *IEEE Trans. Electron Devices* **48** 1844
[22] Brennan K F 1999 *The Physics of Semiconductors with Applications to Optoelectronic Devices* (Cambridge: Cambridge University Press) 512
[23] Kolnik J, Oguzman I H, Brennan K F, Wang R and Ruden P P 1996 *J. Appl. Phys.* **79** 8838